Fracture Mechanics of Concrete Structures
Proceedings FRAMCOS-3
AEDIFICATIO Publishers, D-79104 Freiburg, Germany

WORK OF LOAD VERSUS INTERNAL CRACK GROWTH FOR MORTAR IN COMPRESSION

E. N. Landis and E. N. Nagy
Department of Civil and Environmental Engineering, University of Maine, Orono, Maine, USA

Abstract
A high resolution three-dimensional scanning technique called x-ray microtomography was applied to measure internal damage and crack growth in small mortar cylinders loaded in compression. Tomographic scans were made at different load increments in the same specimen. Three-dimensional image analysis was used to measure internal crack growth during each load increment. Load-deformation curves were used to measure the work of the external load on the specimen. Non-recoverable work of load was related to measured crack growth to estimate work of fracture in three dimensions. Initial results indicate a roughly linear relationship between work of load and internal crack area.
Key words: x-ray, tomography, three dimensional analysis

1 Introduction

1.1 Experimental analysis and fracture
Experimental analysis of fracture properties of heterogeneous materials such as concrete and mortar has been hampered by the difficulty in dealing with non-planar, multiple crack systems that typically characterize the

fracture process. In addition, the measurements made using different experimental techniques can vary considerably depending on the attributes of the particular technique (Mindess, 1990). Experimentalists are often confronted with a trade-off between resolution and field of view. For example, high resolution surface techniques can resolve microcracking and damage to 0.25 μm (Jia and Shah, 1994), however, only the *surface* of the specimen can be observed. Subsurface phenomena are not visible. Acoustic emission techniques allow the inside of the specimen to be examined (Landis and Shah, 1993), however, because it relies on damage generating sufficient energy to be detected as acoustic waves, the resolution is limited.

Because of the lack of good experimentally determined microstructure data, fracture models must be tuned to bulk specimen response rather than changes in the microstructure that ultimately influence the bulk response. Fictitious, effective and smeared crack models are useful for understanding and predicting bulk fracture behavior. However, since they are based only on the very basic principles of physical processes, they often need to be modified to fit new loading or structural configurations. The microstructure processes that ultimately govern fracture behavior tend to be ignored because they are so poorly understood. In describing future research needs, Bazant (1996) emphasized the need for a better micromechanical basis for understanding fracture behavior of concrete. He stated that "understanding of this problem is particularly weak at present." Van Mier (1990) stated that if micromechanics of failure were better understood, the size effects shown in cement-based materials would be dealt with implicitly.

Thus, what is clearly needed to advance our understanding, as well as our modeling abilities is better data relating microstructure to performance properties.

1.2 Experimental approach

In an attempt to advance our knowledge of microstructure-property relationships, a relatively high resolution experimental technique called x-ray microtomography (Flannery et al 1987) was used to image the *internal* structure of mortar cylinders while loaded in compression. Microtomography is similar in practice to conventional CAT-scans used for medical imaging, however, by using a synchrotron x-ray source combined with a high resolution x-ray detector, very high resolution images are possible. The trade-off is that only relatively small specimens can be imaged.

Because we are able to monitor and measure internal processes, we are in a position to make different types of fracture measurements. As described in detail below, we combined external load-deformation data with detailed measurements of internal crack area to investigate work of fracture based only on internal surface area. Because our crack measurements can include the complexities of fracture in heterogeneous materials (tortuous, multiply branched cracks), we are able to free ourselves from such usual simplifications as planar cracks, and two dimensional analysis.

It should be emphasized that the fundamental objective of this work was to explore the possibilities of this experimental technique and the revised definition of work of fracture that it allows, not to make specific work of fracture measurements. The particular experiments were restricted to fracture in compression, as it is perhaps more interesting (and more difficult) than fracture in tension due to the mixed mode nature, and the greater influence of crack branching and multiple crack systems.

2 Work of Fracture

The approach taken for fracture analysis is basic and simple. We simply equated non-recoverable work of load with change in measured internal crack surface area. Specifics terms of the calculations are described in more detail in the descriptions of the experiments, but the idea may be summarized as follows.

The starting point for our work of fracture definition is a basic Griffith-type analysis (Broek, 1986). That is, the total potential energy, Π, of the specimen load system may be written as:

$$\Pi = U - F + W \tag{1}$$

Where U is the internal strain energy, F the external work of load, and W the potential energy associated with crack growth. The condition of crack growth being:

$$\frac{d\Pi}{dA} = 0 \tag{2}$$

or,

$$\frac{dW}{dA} = \frac{d}{dA}(F - U) \tag{3}$$

where dA is an incremental change in crack area, and dW/dA is the work of fracture.

While nearly all energy-based fracture analyses starts with this type of approach, we typically start imposing modifying assumptions, or start working with systems that lead to a simple analysis. For this work we will stop here, and measure work of fracture based more or less on equation 3 as stated. What is different in the analysis conducted here is that we consider dA as the *total* incremental change in crack area measured over the *entire sample*. Because of the three-dimensional nature of the microtomographic data, our area measurement includes all changes in crack area including multiple branching crack systems and tortuousness of crack shapes. The implied assumption here is that all nonrecoverable energy goes into crack propagation. While there is evidence which supports the contrary conclusion, for an initial approximation, we will consider this to be the case. Future work can focus on quantifying the errors associated with this approximation.

Our question, and the basis for these experiments, is how does the non-recoverable work of load, (or the work of fracture, as defined here), vary with crack area if the crack area measurement includes all the multiple branches and tortuousness associated with fracture of a heterogeneous material such as concrete? That is, does concrete really exhibit rising R-curve behavior if we change the way we look at the fracture parameters?

3 Experimental Program

3.1 Experimental details

A set of experiments was set up to measure work of fracture using micro-

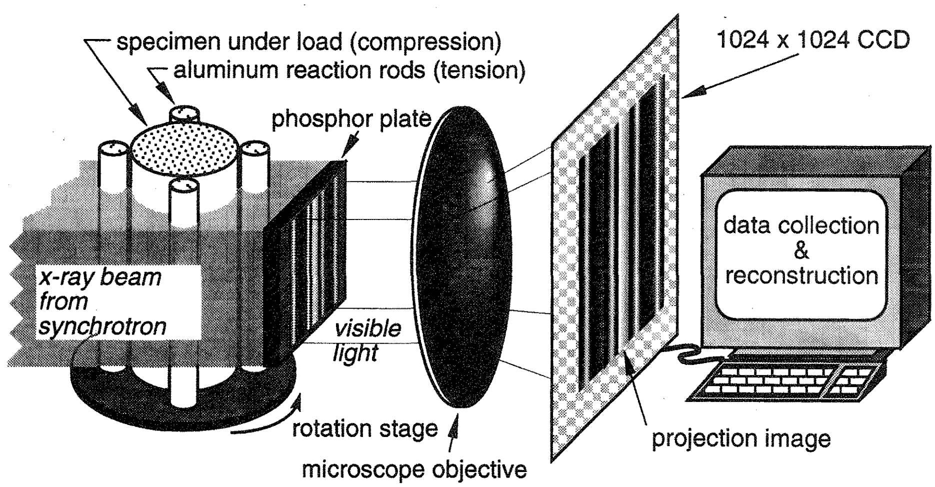

Fig. 1. Illustration of Microtomography Setup

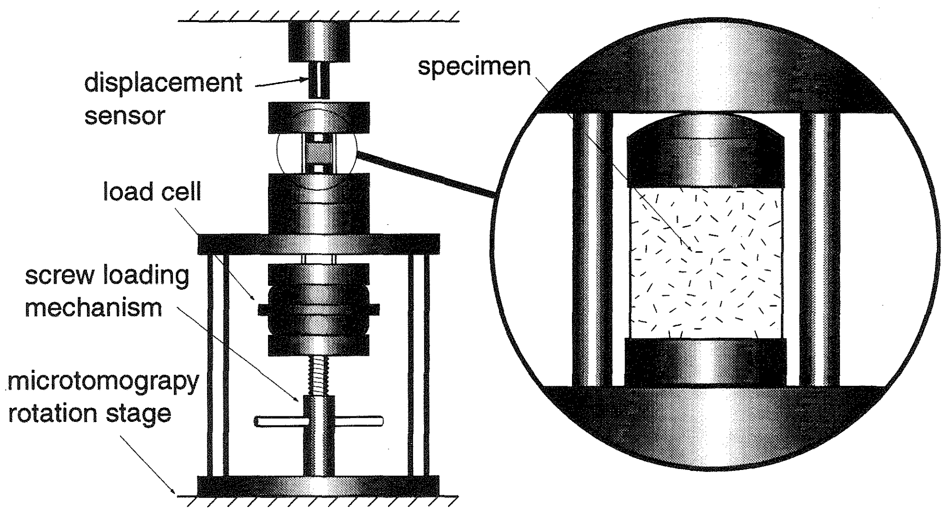

Fig. 2. Loading frame for in situ microtomography scanning

tomography. The basic components of the experiments are illustrated in Figure 1. In addition to the components required for microtomography, a small loading frame capable of applying load to a specimen *while the specimen is being scanned* was constructed. This load frame is illustrated in Figure 2.

The specimens were 4 mm diameter by 4 mm high mortar cylinders having a mix proportion of 1 to 2 to 0.6 parts by weight of type I portland cement to sand (.425 mm max. size) to water. The mix was proportioned to correspond roughly to the mortar phase of a conventional concrete. The small specimen size was dictated by the size of the x-ray beam at the energy level used for scanning.

The general procedure was to place the specimen in the loading frame and mount the loading frame on a rotation stage in the x-ray path. An initial tomographic scan was taken of the undamaged specimen. A compressive load was then applied to the specimen, with the load and displacement continuously recorded, and another scan taken. The cylinder was then unloaded and reloaded to a higher load for another scan. This cycle was continued until after failure. A total of six scans were taken during the loading process, including the baseline case.

3.2 Load-deformation response

The load-deformation response of the specimen was measured in order to calculate work of load and recoverable strain energy as required in equation 3. An experimental complication arose due to the 2 to 3 hours

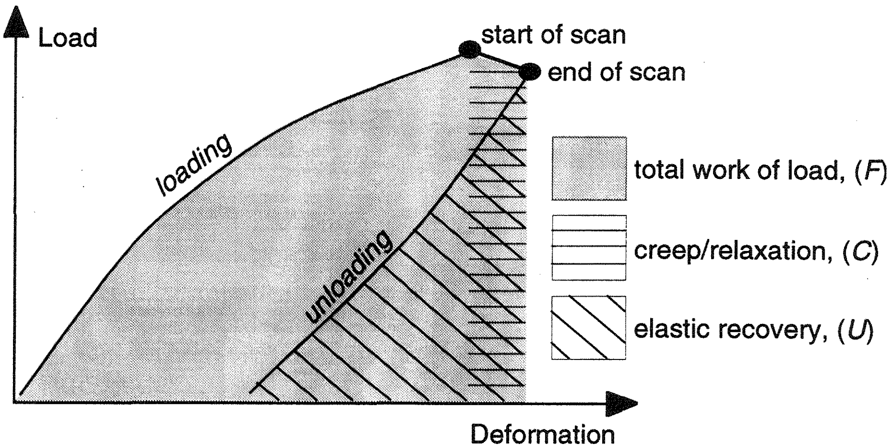

Fig. 3. Illustration of measured load-deformation response

required to complete a tomographic scan. During this time there was measurable creep deformation and corresponding load relaxation at the higher loads. This is illustrated in Figure 3.

Because creep is an inelastic phenomena that does not result from crack growth (at the resolution we are dealing with here), it is not accounted for in equation 3. However, if we assume that creep deformation does not contribute to propagation of cracks, which seems reasonable based on the accepted microstructural mechanisms (e.g. Mindess and Young, 1981), then it can be accounted for through a slight modification of equation 3. If C is the energy dissipated by creep deformation, then we may rewrite equation 3 as:

$$\frac{dW}{dA} = \frac{d}{dA}(F - U - C) \qquad (4)$$

Here F, U, and C are all determined directly from the load-deformation curve as shown in Figure 3. What remains to be determined for evaluating equation 4 is the incremental change in crack area. This is determined through an analysis of the microtomographic images as described below.

3.3 Tomographic images

The microtomographic scans were conducted at the National Synchrotron Light Source (beamline X2B) at Brookhaven National Lab. Beamline X2B was developed by Exxon Research specifically for microtomography.

The microtomography set-up is illustrated in Figure 1. The x-ray beam from the synchrotron ring is monochromated with a silicon crystal to a specific energy. The narrow energy band x-ray then passes through the specimen where it hits a phosphor screen and is converted to visible light. The light is magnified by a microscopic objective (in our case a 2.5X lens system) and then hits a CCD which sends the digitized through-transmission images to a computer for storage and later reconstruction. A total of 720 through-transmission images taken over 180° of rotation were recorded for each scan. The tomographic reconstruction was done using a proprietary program developed by Exxon Research, Inc. The reconstruction produces several hundred cross-sectional "slices" for each scan. A pair of typical reconstructed images is shown in Figure 4. These two images represent roughly the same vertical plane in the same specimen scanned at two different strain levels. The images illustrate how we are able to monitor internal crack growth. Clearly, additional cracking has occurred during the loading increment between the scans from which these images were constructed. It should be noted that the spatial resolution of the images shown is 9.6 μm per pixel on a 544 by 544 pixel image. Again, the specimen shown is about 4 mm diameter.

One of the advantages of a true three dimensional data set is that we are able to view the data in any plane using commercially available three dimensional visualization software. Examples are shown in Figure 5 for a specimen "cut open" along a vertical plane.

While these images illustrate the qualitative assessments that can be made with tomographic data, the real power is in the fact that we may perform quantitative analyses on the various internal features that make up the data sets through image processing techniques as discussed below.

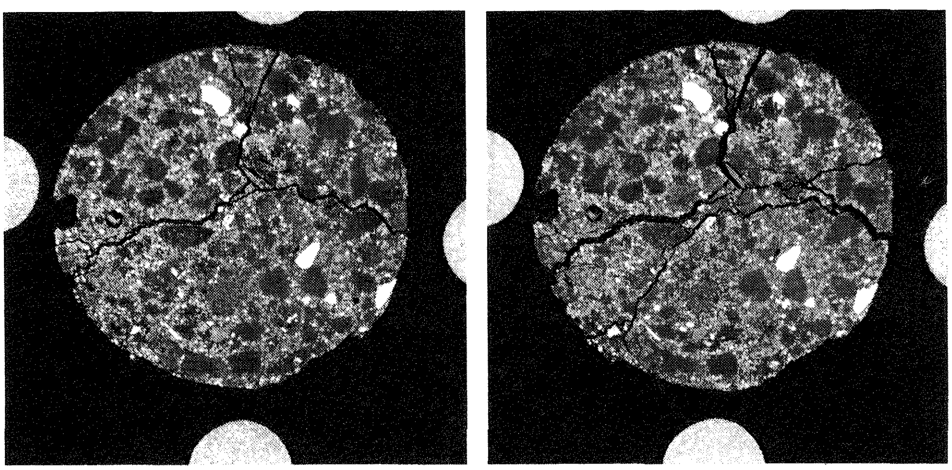

Fig. 4. Typical tomographic images of a specimen at two different loads

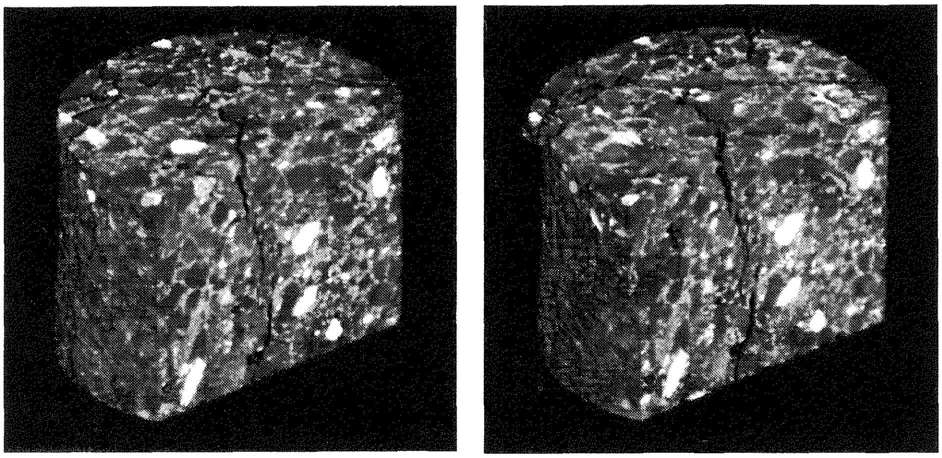

Fig. 5. Three dimensional renderings of tomographic data

4 Data Analysis

4.1 Image processing

The bulk of the data analysis consisted of extracting crack information from a series of image data sets. Even though the process was automated, the job was considerable as each scan produced 512 images at 1024 by 1024 pixels. At two bytes per pixel this amounts to one gigabyte of raw data per scan.

Measuring the surface area of the internal cracks requires three tasks. First the solids (cement and aggregate) must be separated from the air (cracks and voids). Second, the cracks must be identified and labeled as connected components. And third, the crack properties must be measured. A number of sub-tasks were also required, but only the major steps are described here.

First, the images were cropped to 544 by 544 pixels, and the pixel data was scaled from the two bytes that the CCD hardware records, to one byte, that is a more realistic measure of the actual resolution of the measurement. The combination of these two steps reduce the storage requirement by a factor of 7 (from 2 MB per slice to 289 KB per slice).

The second step was a threshold separating air from solid. Although the absolute value of the amount of damage measured for each load is sensitive to the choice of threshold value, preliminary investigations suggest that the *change* in the damage measure between loads is not.

Now that the cracks and voids have been isolated from the solid, they can be labeled and measured. To do this, a three-dimensional connected-

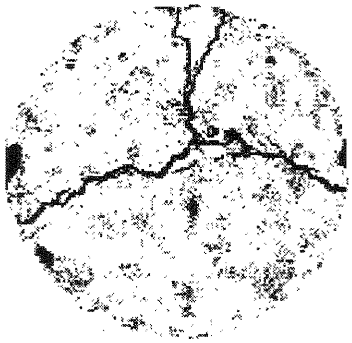

Fig. 6. Example of image processed to isolate cracks and voids from solid.

components routine finds each individual "blob" of air. It does this by scanning through the current slice looking for an unlabeled air pixel. When it finds one, it gives it a label (colors it) and then looks at its neighbors in all three dimensions. Any of its neighbors which is both unlabeled and air colored gets the same label and is put in a list. After it looks at all five neighbors (four in the plane and one below), it goes to the first element in the list, and looks at its neighbors. It continues to go through the list until the list is empty, and then looks for the next unlabeled air pixel in the plane. When it gets to the end of the plane, it starts in the top left corner of the next plane down. In this way, all the cracks and voids in the cylinder are distinguished. Once found, the surface area and volume of each blob can be measured. For this study, the volume was taken to be the number of voxels (3D volume elements as opposed to 2D pixels) that make up the blob, and the surface area is the number of free faces. A cross-sectional slice subjected to this analysis is illustrated in Figure 6. The final step in the analysis is to evaluate total surface area of voids and cracks in each scan, as well as the change in surface area between successive scans, dA, using the connected component data measured in each scan.

4.2 Fracture analysis

Figure 7 shows a plot of the results from a two experiments. The nonrecoverable work of load for each increment was calculated using the terms in the right-hand side of equation 4. The total crack surface area was estimated by counting the number of exposed voxel surfaces on all the connected components. For a first approximation, this number of surfaces was multiplied by 92 square microns, the area of a 9.6 μm by 9.6 μm voxel face.

Actual numerical values of work of fracture are not presented here due to some of the uncertainties associated with this definition of surface area. However, of interest here is the relative shape of the curves. For one

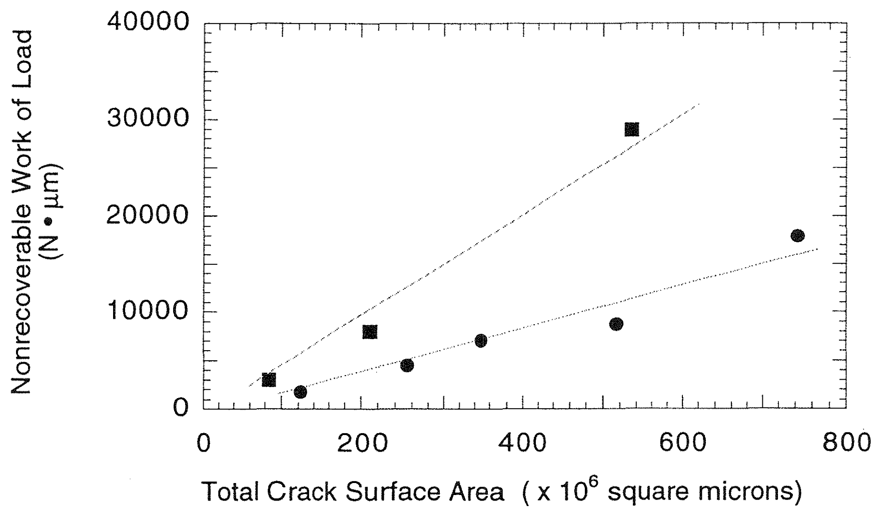

Fig. 7. Plot of nonrecoverable work of load vs. crack surface area

of the specimens in particular, the plot is relatively linear, indicating a constant work of fracture. It is somewhat universally accepted that concrete, being a "quasi-brittle" material demonstrates toughening mechanisms that incrementally increase the work of fracture with increasing crack size, that is, increasing R-curve behavior, (Bazant and Planas, 1997, Shah et al 1996, van Mier, 1997). Our results are not, as it may initially appear, contradictory. It can simultaneously be true that a single crack can exhibit rising R-curve behavior, while a system of many cracks shows a more constant work of fracture. Plotted in Figure 7 is the sum of all cracks in the specimen.

Obviously two specimens are not enough of a sample from which to draw any conclusions, but the initial results present an interesting possibility. Future work will focus on refining the technique and expanding the range of specimens tested.

5 Conclusions

No definitive conclusions about the fracture properties of mortar are made here due to the relative infancy of the experimental technique. The principal conclusion of our work to date is simply that x-ray microtomography can be a powerful tool for investigating fracture energy in complex materials such as concrete. We have shown that using an experimental setup where tomographic scans are made of a specimen under load, changes in internal damage can measured using three dimensional image analysis techniques. When load and deformation data are available, one can make work of fracture calculations for the specimen. Finally we have shown that for a small mortar specimen loaded in compression, we can have a relatively constant work of fracture if we consider the total area of all the crack systems involved.

6 Acknowledgments

This work is supported by the National Science Foundation (CMS-9733769) under a program directed by Dr. John Scalzi. Parts of this research was conducted at the National Synchrotron Light Source, Brookhaven National Laboratory, which is supported by the U.S. Department of Energy, Division of Materials Sciences and Division of Chemical Sciences (DOE contract number DE-AC02-76CH00016.) Additional support of the U.S. Air Force Office of Scientific Research through a program directed by Dr. Michael Chipley is also gratefully acknowledged.

7 References

Bazant, Z. P. and J. Planas (1997). **Fracture Mechanics and Size Effect**. CRC Press, New York.

Broek, D. (1986). **Elementary Engineering Fracture Mechanics**, 4th Edition. Boston, Martinus Nijhoff Publishers, Dordrecht.

Flannery, B. P., Deckman, H. W., Roberge, W. G., and D'Amico, K. L. (1987) Three-Dimensional X-ray Microtomography. **Science**, 237, 1439-1444.

Jia, Z. and S. P. Shah (1994). Two-Dimensional Electronic-Speckle-Pattern interferometry and Concrete-Fracture Processes. **Experimental Mechanics** 34(3): 262-270.

Landis, E. N. and S. P. Shah (1993). Recovery of Microcrack Parameters in Mortar Using Quantitative Acoustic Emission. **Journal of Nondestructive Evaluation** 12(4), 219-232.

van Mier, J. G. M. (1997). **Fracture Processes of Concrete**. CRC Press, New York.

Mindess, S. and Young, J.F. (1981) **Concrete.** Prentice-Hall, Inc., Englewood Cliffs, NJ.

Mindess, S. (1990). The Fracture Process Zone in Concrete. in **Toughening Mechanisms in Quasi-Brittle Materials** (ed. S.P Shah), Kluwer Academic Publishers, Dordrecht, 271-286.

Shah, S. P., S. E. Swartz, et al. (1995). **Fracture Mechanics of Concrete: Applications of Fracture Mechanics to concrete, Rock, and Other Quasi-Brittle Materials**. John Wiley & Sons, Inc., New York.